A COMPARISON OF THREE PROBES USED FOR MEASURING LOCAL HEAT TRANSFER COEFFICIENTS

by

RALPH HUNDLEY BERGSTAD

A THESIS

submitted to

OREGON STATE UNIVERSITY

in partial fulfillment of
the requirements for the
degree of

MASTER OF SCIENCE

June 1962

APPROVED:

Redacted for privacy

Professor of Chemical Engineering

In Charge of Major

Redacted for privacy

Head of Department of Chemical Engineering

Redacted for privacy

Chairman of School Graduate Committee

Redacted for privacy

Dean of Graduate School

Date thesis is presented July 21, 1961

Typed by Margaret Barber

ACKNOWLEDGEMENTS

The writer is privileged to make the following acknowledgements:

To Dr. James G. Knudsen for his encouragement and advice during the course of this research.

To Mr. K. Narayanan for the construction of the experimental equipment and for his help throughout the research.

To the National Science Foundation for financing the project.

To the Department of Chemical Engineering for the use of its equipment and facilities.

TABLE OF CONTENTS

LIST OF FIGURES

LIST OF TABLES

A COMPARISON OF THREE PROBES USED FOR MEASURING LOCAL HEAT TRANSFER COEFFICIENTS

CHAPTER I

INTRODUCTION

The transfer of heat from a hot fluid to a cold fluid is an important industrial operation. The most common type of heat exchanger used in industrial processes is the shell and tube heat exchanger. It consists of a bundle of tubes enclosed in a cylindrical shell. Heat is transferred through the tube wall from the hot fluid to the cold fluid as one fluid flows inside the tubes while the other flows outside the tubes.

To guide the flow of fluid between the outside of the tubes and the shell, baffles are often used. They control the path of the fluid, and they increase the rate of heat transfer between the outside tube wall and the fluid flowing through the shell. The baffles cause the pattern of flow on the shell-side of the heat exchanger to be very complicated. As a result, the rate of local heat transfer varies throughout the exchanger. It is of interest to study local rates of heat transfer in heat exchangers to determine effects of shell-side geometry and local areas of high as well as low heat transfer.

Measurement of local rates of heat transfer have been made by the use of heat transfer sensing probes. The probe usually consists of a heat transfer surface to which heat is supplied. A measure of the heat supplied, the temperature of the heat transfer surface, and the temperature of the fluid give an indication of the rate of heat transfer.

The purpose of the present research was to determine if sensing probes suitable for the measurement of heat transfer rates in a baffled heat exchanger could be developed using the properties of temperature sensitive resistors. Two probes were built using thermistors as the heat transfer surface to which the heat was supplied. The thermistor probes were studied in a model heat exchanger and wind tunnel along with a probe of known characteristics, and the performance of the thermistor probes was determined.

CHAPTER II

THEORY AND PREVIOUS WORK

Conductive Heat Transfer

Conduction is the transfer of heat from one body to another part of a body, under the influence of a temperature gradient, without significant displacement of particles of the body. The mathematical expression for the instantaneous flow of heat $dQ/d\theta$ in one direction is given by Fourier's law

$$dQ/d\theta = -kA\ dt/dx \qquad (1)$$

where A is the area of the section taken at right angles to the direction of heat flow; dt/dx is the rate of change of temperature in the direction of heat flow, and k is a physical property of the material known as the thermal conductivity. When the heat flow is independent of time, the rate $dQ/d\theta$ can be represented by q. Hence, at steady state, Fourier's law becomes

$$q = -kA\ dt/dx \qquad (2)$$

Convective Heat Transfer

Convection is the transfer of heat from one point to another within a fluid, or between a fluid and a solid by movement or mixing of the fluids involved. Heat transfer by convection can be classified as either natural convection or forced convection.

In natural convection, the cool fluid adjacent to a hot surface will become heated by conduction. This causes temperature differences in the fluid, and thereby results in density differences. Because of the density differences, buoyant forces cause a flow of fluid near the surface. Hence, in natural convection the motion of the fluid is entirely the result of differences in density, resulting from differences in temperature.

Forced convection occurs when fluid is forced over a surface which is at a different temperature than the fluid. Heat is always transferred in direction of decreasing temperature. The motion of the fluid in this case is a result of both density differences and the energy supplied to the fluid. Motion due to the former, however, is generally insignificant compared to the latter. Heat is conducted to the adjacent fluid and passes by conduction and convection to the bulk stream.

The heat transfer rate from the surface of a solid to a fluid is defined by

$$q = h_m A(t_w - t)$$

where

q = rate of heat transfer

h_m = mean heat transfer coefficient over the surface area

A = area of surface

t_w = temperature of the surface

t = bulk temperature of the fluid

The coefficient of heat transfer depends on certain physical properties of the fluid, on the velocity of the fluid past the surface, and in many cases on the temperature potential Δt. (8, p.4)

The point or local heat transfer coefficient, h, is given by

$$dq/dA = h(t_w - t) \qquad (4)$$

and is much more difficult to measure than the average coefficient. However, once local heat transfer coefficients are found, they can be used to find mean heat transfer coefficients. Also, since the heat transfer coefficient is a function of fluid velocity local coefficients can be used to study flow patterns over surfaces and show effects of various modes of flow. The importance of being able to measure heat transfer coefficients is apparent.

Methods of Determining Local Heat Transfer Coefficients

Several methods for measuring local heat transfer coefficients have been developed. Each has its specific advantages and disadvantages depending upon the application.

Schmidt and Werner (11, p.3) in studying heat transfer over the circumference of a cylinder used a vapor heated cylinder fitted with an electrically heated copper bar. A hollow brass cylinder was kept at a constant temperature by internal heating with vapor, except at one place where a strip of the surface was removed and replaced by a hollow copper bar that was heated internally by electricity. This heating element was insulated by an air layer bounded by polished metal surfaces. The electric heating of the copper bar was so adjusted that it assumed the same temperature as the vapor heated cylinder. The power input to the heating coil, the temperature of the copper surface, and the air stream temperature were measured. With these and the surface area of the copper bar, a local heat transfer coefficient was calculated. This is not a local heat transfer coefficient in the sense of a point coefficient but an average coefficient over the area of the copper.

In determining heat transfer rates of water through a tube bank, Dwyer (3, p.6) used nickel tubes that were heated electrically by their own resistance using a high amperage low voltage current. The radial heat flux from a

given tube was determined from the voltage drop across the section of the tube in the flowing stream. The heat transfer coefficient was determined by measuring the total temperature difference between the inside wall of the tube to the bulk water temperature. An expression was derived relating power input, inside wall temperature, radius of the tube, and bulk water temperature to the heat transfer coefficient. The inside wall temperature was measured at various fixed angles around the circumference of the tube by a revolving pin point thermocouple probe. In calculation of the heat transfer coefficient, the nickel tube was treated as a hollow cylinder with an adiabatic inner surface, and heat generation was assumed uniform.

Hardwick, Barsch, and McDonald (6, p.239) developed a heat meter which is a thermopile on a miniature scale. The meters were wound on a glass core 0.007 inches by 1/16 inch by 1/8 inch. Fifty turns of 0.001-inch constantan wire spaced 0.001 inches apart were wound on the core. Then the long edge of the meter was immersed in a silver plating solution so one half of each loop was plated. Thus an effective silver-constantan junction was formed on each loop at the center of the two flat sides of the meter. The meter was then coated with a thin high temperature cement to prevent shifting of the wires. A model to be studied was coated with 0.02 inches of porcelain, and a

small indentation was made into which the meter was placed. The surface was smoothed over, and connections were made by silver paint to wires at the rear of the model. Since the sensitivity of a meter is greatly affected by the method of installation and the thermal conductivity of the material into which it is installed, the meters must be calibrated. Calibration was carried out in an oven, and a plot of heat flux versus millivolts was used for a calibration curve. The meters have been used for heat transfer studies at very high fluid velocity rates, seven to eight times the speed of sound.

Zapp (14, p.23) measured local heat transfer coefficients around a cylinder by measuring the condensation rate of steam in a thermally insulated segment of a two-inch pipe. A small segment four inches long by 0.38 inches wide was machined from the pipe and replaced by a thermally insulated section in the form of a small steam chest to which steam could be supplied and condensate collected. The pipe itself was maintained at a constant temperature by the passage of steam through it. Measurement of the condensation rate, the temperature difference between the condensing steam and the flowing air, and the area of the insulated section gave a value for the local heat transfer coefficient.

Winding and Cheney (13, p.1087) used the analogy between heat and mass transfer in studying the heat transfer coefficients in tube banks. Naphthalene tubes were cast and inserted into various positions in the tube bank. Air was passed through the tube bank, and mass transfer coefficients could be obtained from the loss in weight and change in dimensions of the naphthalene tubes. Heat transfer coefficients were calculated by use of the Chilton and Colburn analogy for transfer of heat and mass. The Chilton and Colburn analogy can be expressed as follows:

$$j_D = j_H$$

where

$$j_H = h/C_pG\ (C_p\mu/k)^{2/3}$$

for heat transfer, and

$$j_D = \frac{KP}{G/M}\ \left(\frac{\mu}{\rho\, k_d}\right)^{2/3}$$

for mass transfer.

The nomenclature is as follows:

h = heat transfer coefficient

C_p = specific heat of flowing fluid

G = mass velocity of flowing fluid

ρ = density of the flowing fluid

μ = viscosity of flowing fluid

P = total pressure

k = thermal conductivity of flowing fluid

K = molar mass transfer coefficient

M = molecular weight of naphthalene

k_d = diffusion coefficient of naphthalene

All the factors in the j_D expression are known or can be measured, and the only term unknown in the j_H expression is the heat transfer coefficient. Hence, the heat transfer coefficient can be calculated.

Giedt (3, p.375) used a heated resistance ribbon technique to study point heat transfer coefficients around a cylinder normal to an air stream. A thin nichrome foil wound helically around the cylinder was electrically heated. Point heat transfer coefficients were determined from the temperature of the ribbon, and the electrical input to the ribbon. The temperature of the ribbon was measured by means of very fine thermocouples. Short lengths of iron and constantan wire were spot welded to the nichrome ribbon before it was placed around the cylinder. The wires were lead through the cylinder wall and soldered to leads brought in through one end of the cylinder. To reduce conduction losses the cylinder was filled with glass wool. By making an energy balance on a differential piece of ribbon, an expression for the local heat transfer coefficient was derived. Measurement of the air temperature, ribbon

temperature, and power input to the ribbon were sufficient to calculate the heat transfer coefficient. Estimates of conduction losses and radiation losses were also made.

Ambrose (1, p.41) constructed a heat transfer sensing probe based on the heated foil principle used by Giedt. The probe was used to study local heat transfer coefficients inside a model heat exchanger. The sensing probe was made from a six-inch piece of one-inch lucite plastic rod. Seven iron-constantan thermocouples were placed in a groove around the circumference of the rod. Next a layer of "Saran Wrap" was placed over the thermocouples to keep them from shorting out on the heating foil. The heating foil was made of nichrome resistance ribbon, and three strips were placed adjacent to each other on the probe. The center foil was placed over the thermocouples. The rod was grooved longitudinally, and small copper bars were screwed in the grooves to hold the foil in place and to serve as a junction between the power leads and the foil. The foils were heated by direct current, and the thermocouple readings were taken with a potentiometer. Radiation losses were estimated as being small and were not considered in the calculation of local heat transfer coefficients. The probe developed by Ambrose has been used extensively in the measurement of local heat transfer coefficients in heat exchangers.

Gould and Nyberg (5, p.249) used a small thermistor embedded in a plane surface for measuring viscous heating and microstreaming effects. The resistance of the thermistor was measured by attaching its leads to a Wheatstone bridge so that the thermistor became one of its arms.

The bridge can be used in two ways. The current through the thermistor can be kept small. The heating is then negligible, and at equilibrium, the temperature of the thermistor is that of the surroundings. The current can also be made relatively large so that self-heating of the thermistor occurs. The temperature is controlled by the rate at which heat is transferred to the surroundings. It can therefore be used to measure heat transfer rates.

Operation of Thermistors

Thermistors are temperature sensitive resistors and have been used extensively as temperature control devices. The two properties of thermistors that are of interest in measuring heat transfer coefficients are their ability to measure small changes in temperature, and their ability to dissipate heat to the surroundings when sufficient current is passed through them. (2, p.711)

Most thermistors are semiconductors. A semiconductor is a material whose electrical conductivity at or near room temperature is much less than that of a typical metal, but

much greater than that of an insulator. The specific conductivity is defined as the reciprocal of the specific resistance which is defined as

$$R = \rho L/A \qquad (5)$$

where

R = resistance

A = cross-sectional area of material

L = length of material

ρ = specific resistance

The specific resistance is dependent upon the material and is a function of temperature. For metals which are conductors, a good approximation for the specific resistance as a function of temperature is as follows:

$$\rho = \rho_o + \alpha(T-T_o) \qquad (6)$$

where

ρ_o = specific resistance at temperature T_o

T = absolute temperature

α = temperature coefficient of resistivity

The temperature coefficient of resistivity is defined as

$$\alpha = 1/\rho \ d\rho/dT \qquad (7)$$

and for a conductor such a platinum is +0.0037 at 300°K.

The relationship between specific resistance and temperature is much different for a semiconductor. If a plot of reciprocal temperature versus the logarithm of specific resistance is made, an almost straight line results. Putting this into a mathematical expression

$$\rho = \rho_\infty e^{\beta/T} \qquad (8)$$

where

ρ_∞ = specific resistance when 1/T equals 0

β = slope of the line

It follows from equation (7) the temperature coefficient of resistivity for a semiconductor is

$$\alpha = -\beta/T^2 \qquad (9)$$

For a typical semiconductor material of which thermistors are made α has a value of -0.044 at 300°K. This is roughly 10 times larger than that for a conductor and opposite in sign.

In measuring temperatures the current through the thermistor must be kept small so that there is no appreciable heating. The temperature of the thermistor is then that of its surroundings. Since the resistance is a function of temperature a measure of the resistance will give from equation (8) the temperature of the thermistor.

When current is applied to the thermistor, power equivalent to the product of voltage and current is generated.

$$P = VI = I^2R \qquad (10)$$

where

V = voltage across the thermistor

I = current through the thermistor

As the current assumes larger values, the power dissipated increases; the resistance decreases, and hence, the voltage is less than it would be if the resistance had remained constant. Figure 1 shows the relationship between thermistor current and voltage. The numbers on the curve indicate the temperature rise above ambient for the thermistor.

It appears from the properties of thermistors that they would be satisfactory in studying heat transfer coefficients. They have a fast response time, are sensitive to temperature, and can be used to measure heat losses. Thermistors are made in a variety of shapes and sizes, and there should be little trouble mounting them in a probe. A measure of the thermistor temperature, the air temperature, and power input to the thermistor will give an indication of the heat transfer coefficient if the thermistor itself is used as the heat transfer surface.

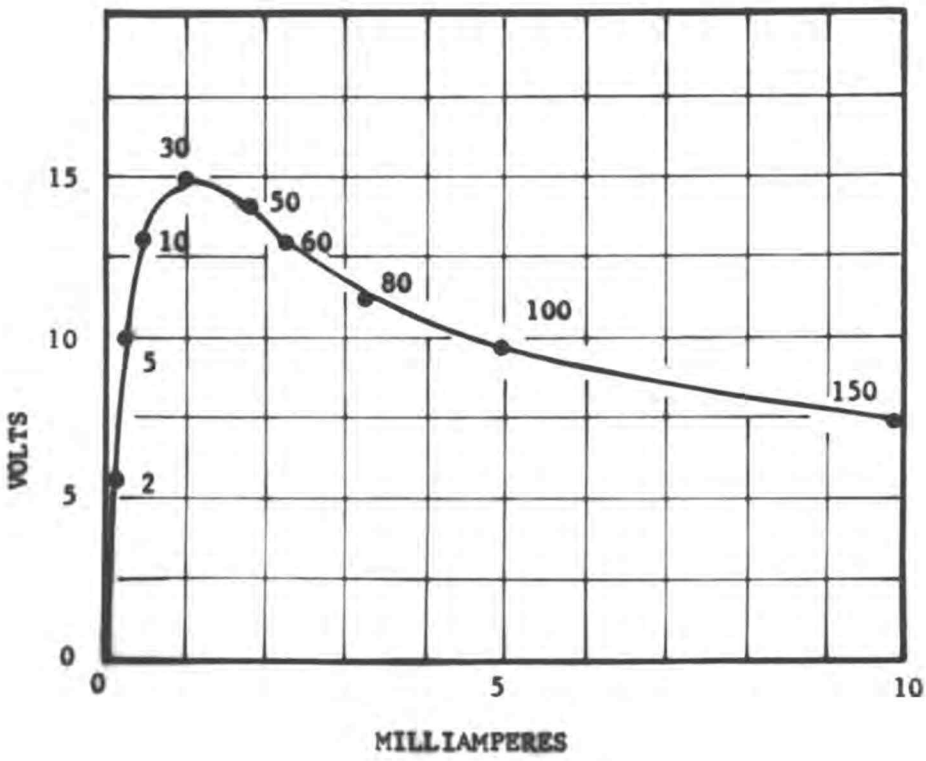

CURRENT VERSUS VOLTAGE
FOR A TYPICAL THERMISTOR

FIGURE 1

CHAPTER III

EXPERIMENTAL APPARATUS

The essential experimental equipment consisted of three heat transfer sensing probes, an air source, the power supplies for the probes, and the electrical measuring equipment.

The Standard Probe - Probe A

The standard probe used the heated foil principle and was similar in construction to that used by Ambrose. (1, p.41) Thermistors were used in place of thermocouples for measuring the foil temperature.

The probe consisted of two sections of 3/4-inch lucite plastic rod which could be screwed together. A 3/16-inch hole passed longitudinally the length of the probe. When the probe was assembled, it was eight inches long. A 3/16-inch plastic spacer was located between the two probe sections, and the thermistors were embedded at 45° intervals around the probe at the junction of the spacer and one section of the probe. Three grooves, 0.002 inches deep and one inch wide, were machined 1/4 inches apart around the circumference of the probe. The foil was placed in these grooves and fastened to the plastic by means of copper bus bars which fitted in slots that were machined longitudinally

on the probe. The bus bars were attached to the probe by machine screws and so arranged that the three foil strips could be connected in series.

Leads from the thermistors and the power leads from the bus bars passed through the center of the probe and through a 3/4-inch aluminum mounting tube to a plug socket and terminals. The thermistor leads were soldered to an eight pin plug, and the two power leads were attached to terminals to which the power supply could be attached. Lead wires for the thermistors were 29-gauge double cotton covered copper wire. The power leads were 12-gauge insulated copper wire.

Seven thermistors were used to measure the foil temperature. The thermistors were Keystone type L-0503-56K thermistors and had a resistance of 56,000 ohms $\pm$ 10 per cent at 37.8°C. The three foils were nichrome resistance ribbon having the trade name "Tophet C". The foil was one inch wide and 0.002 inches thick and had a specific resistance of 0.263 ohms per foot and thermal conductivity of 7.63 Btu/hr. $ft.^2$ $^{\circ}F/ft.$ Probe A is shown in Figure 2.

Heated Bead Thermistor Probe - Probe B

Probe B was similar to Probe A except that no foil was used. Power was supplied directly to the thermistors, and

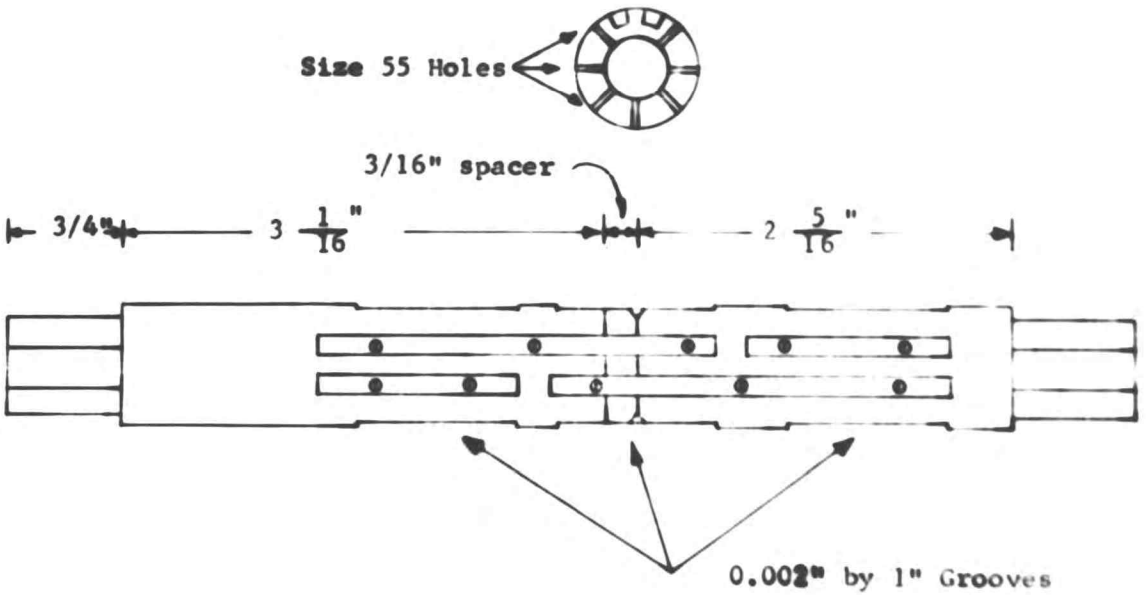

DRAWING OF ASSEMBLED PROBE "A"

FIGURE 2

the thermistors themselves were used as the heat transfer surface and the temperature sensing elements.

The probe consisted of two hollow sections of 3/4-inch lucite rod that could be screwed together. A 1/2-inch spacer was placed between the two sections of the probe, and when assembled, the probe was 6 1/2 inches long. Eight No. 55 holes were drilled at 45° intervals around the spacer. The areas of the holes were measured with a microscope and are listed in Table II in the appendix. The thermistors were placed in the holes, and one lead of each thermistor was taken out on each side of the spacer. A copper ring acted as a common terminal for one set of thermistor leads while the other leads were attached to separate terminals on the other side of the spacer. No. 60 holes were drilled in the threaded section of the probe. Copper lead wires, 29-gauge double cotton covered, were threaded through the probe, through the No. 60 holes, and attached to the terminals of the spacer. Another lead was connected to the copper ring. The probe was assembled by screwing the two probe sections together thus clamping the spacer between them.

The probe was mounted to a 3/4-inch aluminum tube. The lead wires were passed through the tube and soldered to an 11 pin plug. The surface where the thermistors were embedded in the plastic was made smooth by covering the

discontinuities with a conductive putty made from silver dust and ordinary glue. Area of the heat transfer surface of each thermistor was considered to be the area of the hole in which the thermistor was embedded.

The thermistors used in this probe were the same as those used in Probe A. A drawing of Probe B is shown in Figure 3.

Heated Washer Thermistor Probe - Probe C

Probe C operated on the same principle as Probe B but was designed to measure average coefficients around the tube.

The probe consisted of two hollow sections of 3/4-inch lucite rod that could be screwed together. A washer type thermistor placed between two copper washers was mounted between the probe sections. A lead wire from each copper washer was passed through the probe and an aluminum mounting tube and connected to a terminal strip fastened to the end of the tube.

The thermistor was a General Electric W 751 washer thermistor and had an outside diameter of 0.750 $\pm$ 0.001 inches. A drawing of the probe is shown in Figure 4. A photograph of all three probes mounted in their aluminum tubes is shown in Figure 5.

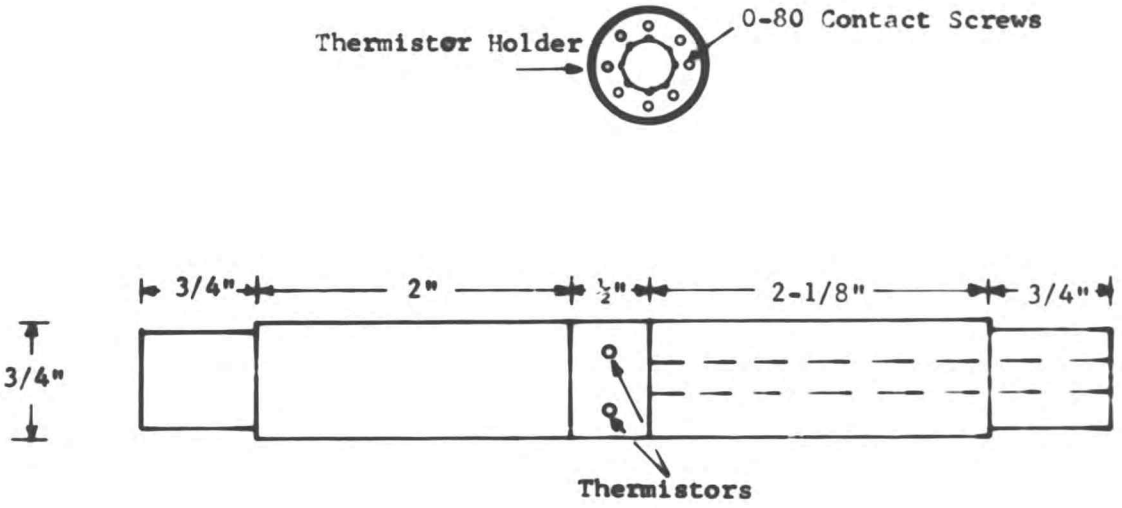

DRAWING OF ASSEMBLED PROBE "B"

FIGURE 3

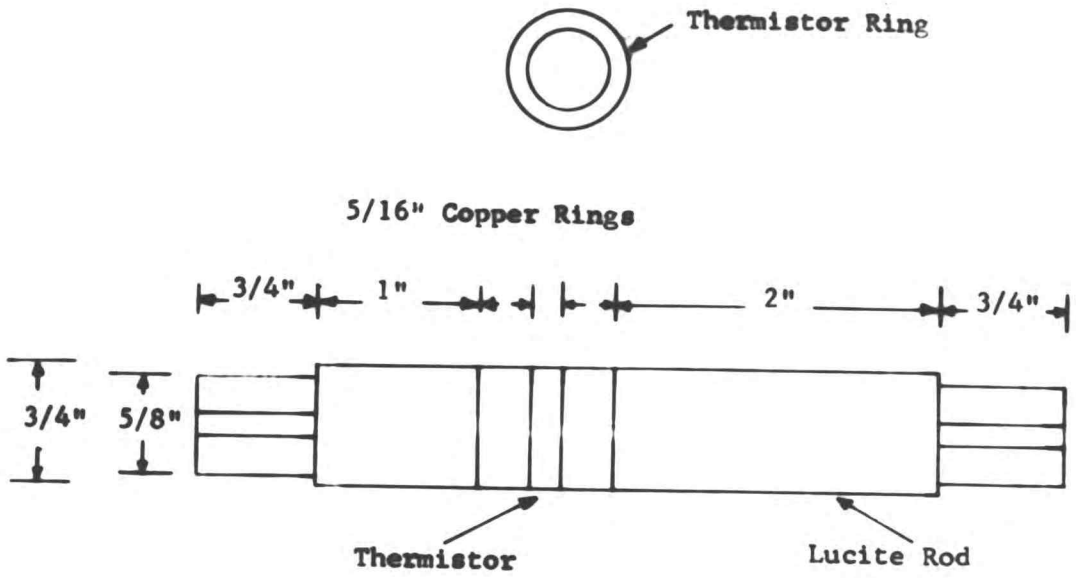

DRAWING OF ASSEMBLED PROBE "C"

FIGURE 4

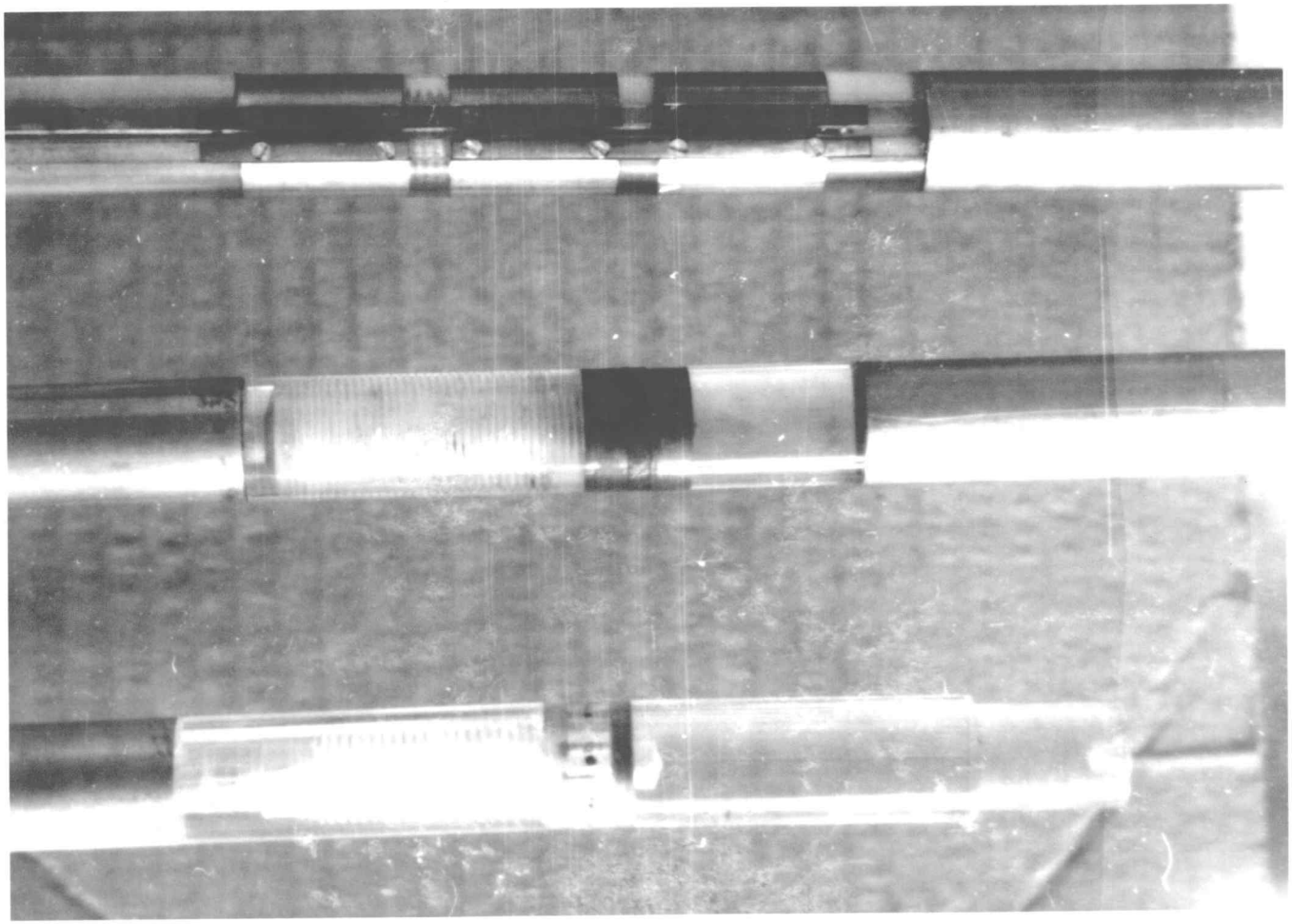

FIGURE 5

Power Supplies

All of the probes used direct current. Probe A required a relatively large amount of power as compared to Probes B and C. For Probe A the power supplied to the resistance ribbon was of the order of 60 watts, while that supplied to Probe B was only 0.2 watts, and that for Probe C was about 1.0 watt.

The power supply for Probe A was a 12-volt battery charger and associated equipment. The 110-volt alternating current power supply to the battery charger was stabilized by a Raytheon (No. VR-6173) voltage stabilizer. Direct current output from the battery charger passed through a rheostat which permitted adjustment of power to the probe heating foils. A 0 to 10 range ammeter accurate to ± 0.1 amperes was used to measure the current to the resistance ribbon. A switch, 0 to 10 range voltmeter accurate to ± 0.1 volts, and a pilot light completed this portion of the circuit.

For Probe B the power was obtained from a Westinghouse "Rectax" power pack which was rated at 750 watts. Line voltage was supplied to the power pack through a variable auto transformer. The current from the power pack passed through a capacitive input filter, and the output was metered by a 0 to 25 range voltmeter which had an accuracy of ± 0.2 volts. The eight thermistors were in parallel,

and a 0 to 1 milliammeter with an accuracy of ± 0.01 milliamperes was placed so that it could measure the current through each thermistor by means of a switching arrangement. A circuit diagram is shown in Figure 6.

The power for Probe C came from the Westinghouse power pack and passed directly through a rheostat. The rheostat was used to adjust the power input through the thermistor. The measuring apparatus consisted of a 0 to 30 range voltmeter with an accuracy of ± 0.5 volts and a 0 to 150 milliammeter with an accuracy of ± 2 milliamperes.

Resistance Measuring Equipment

The foil temperature on Probe A was determined by measuring the resistances of the thermistors under the foil. This was done by using the Wheatstone bridge shown in Figure 7. One leg of the bridge contained a set of variable resistors, another leg the thermistors, and the last two legs the fixed ratio resistors. A microammeter was used as a null dector. Input from the thermistors was through a 15 pin connector and was selected by an 11 position switch. In the range concerned, the accuracy of the resistance measurement is ± 10 ohms. This corresponds to a change in temperature of ± 0.01°F.

Probes B and C required only the already mentioned voltmeter and ammeter for measurement.

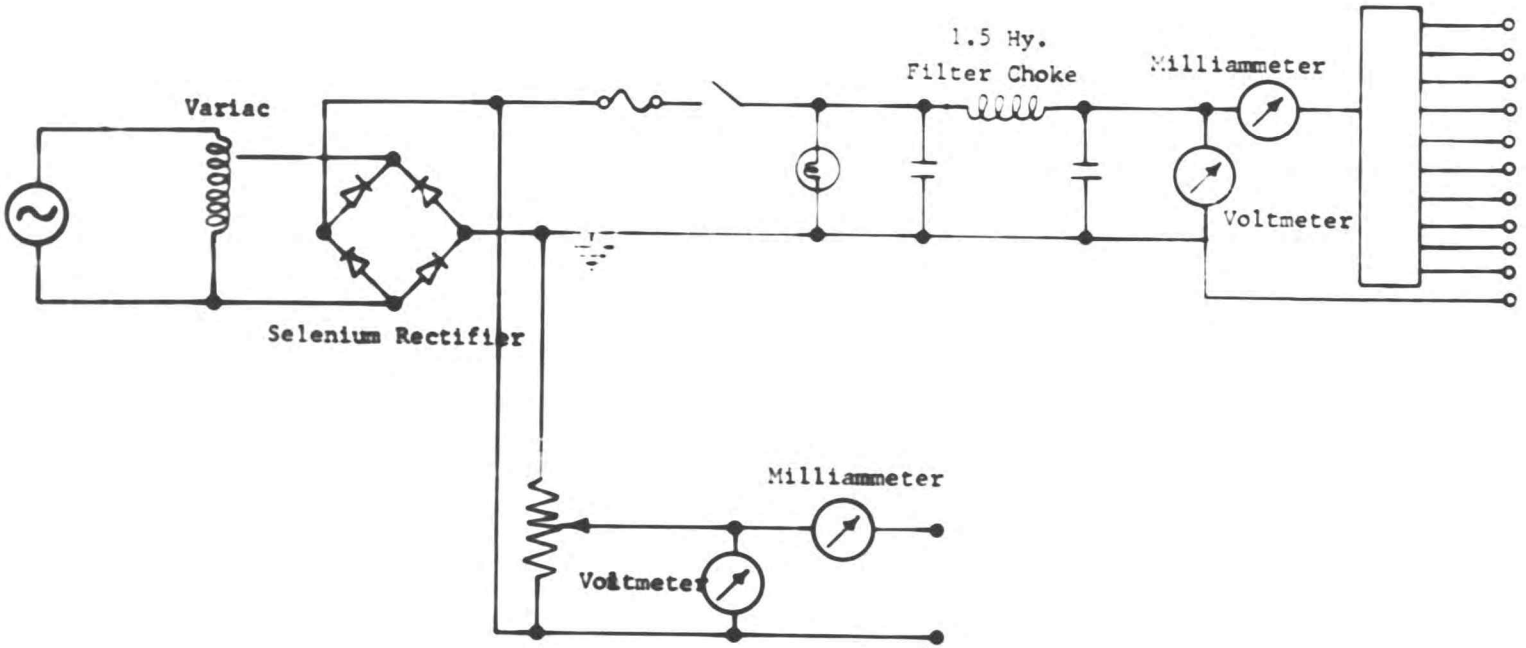

POWER SUPPLY FOR PROBES "B" AND "C"

FIGURE 6

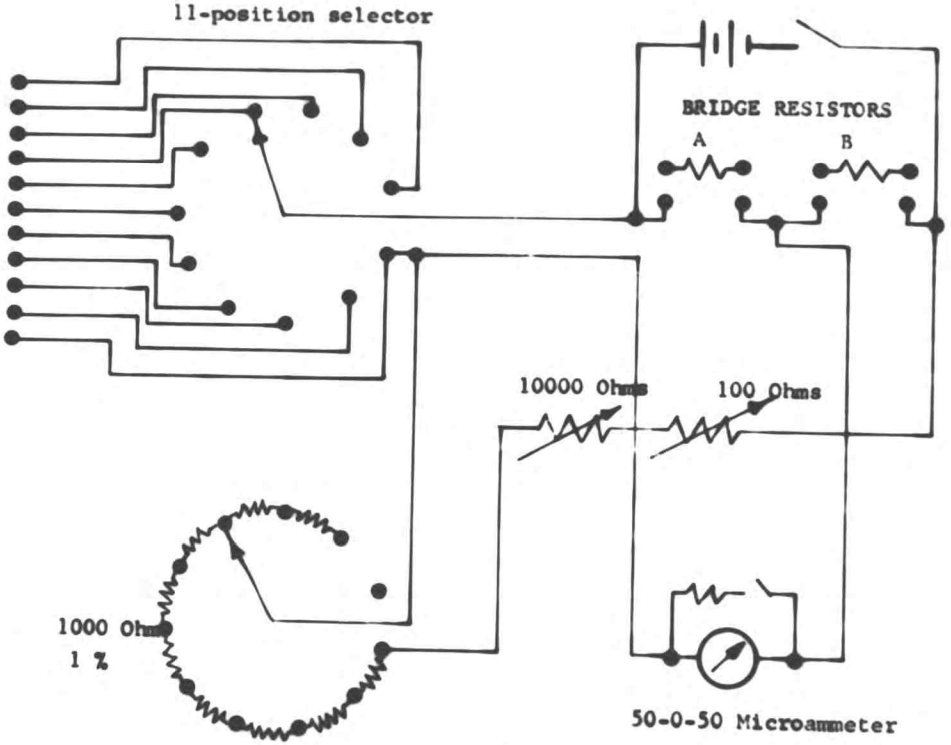

DIAGRAM OF RESISTANCE MEASURING EQUIPMENT

FIGURE 7

Air Source

Air was used as the cooling fluid for the probes. The air was forced over the probes at different flow rates in order to change the heat transfer coefficients. The heat transfer coefficient measured by the standard probe was then related to measurements made by the other two probes.

Two different air sources were used. During the first set of calibration measurements, the probes were placed in symmetrical positions in a baffled multitube model heat exchanger. The flow pattern on the shell side of such a heat exchanger is complicated, and there is considerable variation in the coefficient throughout the exchanger. The probes were calibrated by placing them in positions which were geometrically identical in the exchanger, and hence, the same flow conditions and therefore the same heat transfer coefficients existed at each probe.

Air was supplied to the heat exchanger by a Roots type blower with a rating of 280 cfm at 3 1/2 psig outlet pressure. The hot air leaving the blower was cooled in water coolers to about room temperature before it passed to the exchanger. The probes were mounted between two aluminum heat exchanger tubes and could be moved anywhere along the tube position.

A second test of the probes was made in a wind tunnel capable of a maximum air flow rate of 950 ft/min through a test section two feet by two feet by eight feet long. By partially covering the fan intake, flow rates between 50 feet per minute and the maximum were obtained. The probes were mounted between two pieces of aluminum heat exchanger tubing and placed in the tunnel so flow would be parallel to the probes. The tubes were fastened to a solid support three feet downstream from the probe. On the upstream end of the probe was a 16-inch piece of 3/4-inch aluminum tube. A six-inch piece of wooden dowel with a rounded end was placed in the end of the tube. Probe A was placed approximately in the center of the test section, and Probes B and C were placed five inches on either side of it. The flow pattern across the wind tunnel was checked with a velometer and was found to be approximately uniform across the section where the probes were mounted.

CHAPTER IV

EXPERIMENTAL PROGRAM

The experimental program was designed to calibrate the probes over a large range of heat transfer coefficients. Since Probes B and C were designed to be used in the model heat exchanger they were placed in the exchanger in geometrically similar positions, and comparative measurements were taken with all three probes. The flow patterns in the baffled heat exchanger are such that a fairly wide range of heat transfer coefficients exist throughout the exchanger.

Heat transfer coefficients were measured with all three probes at various positions in the model heat exchanger. The heat exchanger contained orifice baffles, and the local heat transfer coefficients around the tube were fairly constant because of the longitudinal flow existing in the exchanger. This is in agreement with an investigation of orifice flow patterns made by Williams. (12) Probes B and C were run in geometrically similar positions as Probe A so that they would be subjected to the same flow patterns, and hence, the same heat transfer coefficients.

Another set of tests was made on Probe C in the wind tunnel. The air flow rate through the wind tunnel was

changed to obtain a variation of heat transfer coefficient. The flow rate was changed over the same range with two different power inputs to Probe C. Another reading was taken at still a lower power input at the maximum flow rate in the tunnel.

CHAPTER V

EXPERIMENTAL PROCEDURE

The experimental procedure used for measuring the heat transfer coefficients in the model exchanger required the following steps:

1. Install the probes to be studied and the standard probe in geometrically similar positions in the heat exchanger.
2. Open the bypass line from the blower and close the line to the heat exchanger.
3. Turn on the cooling water for the exchangers used to cool the air leaving the blower.
4. Start the battery charger by turning on the timer.
5. Connect voltage stabilizer to wall outlet.
6. Start the blower.
7. Open the line to the test section and partially close the bypass.
8. Switch on Probe A Direct current power source.
9. Adjust Probe A rheostat to obtain the desired current.
10. Turn on variable auto transformer to supply power to power pack.
11. Adjust voltage to Probe B to desired value with variable auto transformer.

12. Adjust rheostat for Probe C to the desired voltage reading.
13. Let all three probes reach equilibrium.
14. Record voltage and current readings for Probes B and C and the resistance readings for Probe A.
15. Reposition the three probes and repeat steps 13 and 14.

The procedure used for the wind tunnel test was the same, except instead of repositioning the tubes, the flow rate through the wind tunnel was changed.

CHAPTER VI

CALCULATION OF EXPERIMENTAL DATA

Probe A

The local heat transfer coefficients for Probe A were calculated from the temperatures measured by the thermistors, the air temperature, and the current input to the resistance ribbon. All computation was done using the Alwac III-E computer.

The equation used for the calculation of the heat transfer coefficients was derived by Ambrose. (1, p.79) This equation was derived by making an energy balance on a differential element of the nichrome resistance ribbon. Since the two ribbons adjacent to the center ribbon were also heated, the amount of longitudinal conduction was reduced and the longitudinal temperature variation of the center foil was considered negligible. In the derivation, the amount of heat lost by conduction into the plastic and by radiation were shown to be sufficiently small so that they could be neglected.

A heat balance on a small element of ribbon yields the following:

(heat conducted in) + (heat generated) = (heat conducted out) + (heat convected to the fluid) + (heat radiated to the surroundings) + (heat

conducted into the plastic center of the probe)

Neglecting the last two items, this energy balance yields the following equation.

$$-kzw\, dt/dS + i^2 R dS = -kzwd\left[t + \left(\frac{dt}{dS}\right) dS\right] + h\, wdS(t-t_a) \qquad (11)$$

where

S = length of resistance ribbon

z = thickness of resistance ribbon

i = current through resistance ribbon

R = resistivity of the resistance ribbon

t = temperature measured by thermocouples

t_a = air temperature

h = local heat transfer coefficient measured by Probe A

k = thermal conductivity of the ribbon

w = width of the resistance ribbon

solving for h gives

$$h = \frac{\frac{i^2 R}{w} + \frac{kzd^2 t}{dS}}{t - t_a} \qquad (12)$$

Since $S = r\phi$ where ϕ equals the enclosed angle in radians

$$dS = r\, d\phi \qquad (13)$$

and

$$\frac{dt}{dS} = \frac{dt}{r d\phi} \tag{14}$$

Differentiating with respect to S

$$\frac{d^2t}{dS^2} = \frac{d^2t}{r d\phi dS} \tag{15}$$

Substituting (12) into (14) there results

$$\frac{d^2t}{dS^2} = \frac{d^2t}{r^2 d\phi^2} \tag{16}$$

Substituting (16) into (12) the final expression for the heat transfer coefficient is obtained.

$$h = \frac{\frac{i^2R}{w} + \frac{kz}{r^2}\frac{d^2t}{d\phi^2}}{t - t_a} \tag{17}$$

The following constants are known.

R = 0.263 ohms/ft.

w = 1.00 inches

k = 7.63 Btu/hr. $ft.^2$ $^oF/ft.$

z = 0.002 inches

r = 0.375 inches

When the above quantities are substituted into (17) and ϕ is changed to degrees, the following results.

$$h = \frac{10.77i^2 + 4276 \frac{d^2t}{d\phi^2}}{t - t_a} \qquad (18)$$

This equation was programmed for the Alwac III-E computer and used to calculate the local heat transfer coefficients from the resistance and current readings.

The average heat transfer coefficient around the tube was calculated by averaging the local coefficients calculated from equation (18).

$$h_A = 1/7 \sum_{1}^{7} h_i \qquad (19)$$

where h_i is the coefficient at a thermistor.

The temperatures used in computing the heat transfer coefficients were calculated from the resistances of the thermistors by the following equation.

$$R = R_o e^{\beta(1/T - 1/T_o)} \qquad (20)$$

where

R = resistance of thermistor at temperature T

R_o = resistance of thermistor at temperature T_o

e = 2.718

β = constant

The constant depends upon the material in the thermistor. The seven thermistors used for Probe A were calibrated by measuring their resistances at 560 ^{o}R. Table I in the appendix lists resistances of the thermistors, the temperature, and the value of which was given in the manufacturer's specifications.

Probe B

Since the same type of thermistors were used for Probe B, the same value of was also used. To simplify the calculations, the thermistors were reduced in size with ordinary sandpaper until each thermistor had approximately the same resistance at the same temperature. At 560 ^{o}R all thermistors had a resistance of 58,000 ± 200 ohms. Substituting into equation (20)

$$R_B = 58{,}000\, e^{7750(1/T - 1/560)} \qquad (21)$$

An energy balance on a single bead thermistor results in the following equation.

(electrical heat input) = (heat lost by conduction into plastic) + (heat lost by convection) + (heat lost by radiation)

This becomes

$$q = hA(t-t_a) - k\,\bar{A}\left(\frac{\partial t}{\partial r}\right)_{r=r_w} + \epsilon\sigma A\,(T^4 - T_a^4) \qquad (22)$$

where

k = thermal conductivity of the plastic

$\bar{A}$ = conduction area

$\left(\frac{\partial t}{\partial r}\right)_{r=r_w}$ = temperature gradient between the plastic and the thermistor

σ = Stefan-Boltzman constant

ϵ = emissivity of the radiating surface

t = temperature of the surface of the thermistor

t_a = air temperature

q_B = heat input to a Probe B thermistor

Grouping the conduction and radiation terms together as losses, the following is obtained.

$$q_B = hA(t - t_a) + \text{losses} \qquad (23)$$

The heat inputs to the thermistors were calculated from the voltage and current readings of the thermistors.

$$q_B = VI\ (3.413\ \text{Btu/ hr. watt}) \qquad (24)$$

In equation (22) the unknown quantities are the heat transfer coefficient and the losses due to radiation and

conduction. If the losses are small, a good indication of local heat transfer coefficient can be calculated by

$$h_B = \frac{q_B}{A_B(t_B - t_a)} \qquad (25)$$

and comparison with heat transfer coefficients from Probe A will permit an estimation of the losses. If the losses are large, possibly a calibration could be made between Probe A and Probe B so that the latter could be used satisfactorily. It would be desirable to use Probe B because of its small power requirements and rapidity with which it reaches equilibrium.

Probe C

The thermistor washer of Probe C had a value of 7150 ^{o}R as given by the manufacturer. The constants R_o and T_o in equation (20) were determined by measuring the resistance of the thermistor at room temperature which was found to be 482.7 ohms $\pm$ 0.1 ohm. The following equation was used to compute the temperature of the thermistor from its resistance.

$$R_C = 482.7 \; e^{7150\,(1/T - 1/539)} \qquad (26)$$

An energy balance on the thermistor results in an expression similar to that for Probe B.

$$q_C = hA(t - t_a) + \text{losses} \qquad (27)$$

where q_C is the heat input to the washer thermistor and is calculated from equation (24).

Since thick copper rings were located on each side of the thermistor, conduction into the copper would be considerable. With the known heat transfer coefficient from Probe A, a calibration may be obtained by calculating a fictitious heat transfer coefficient neglecting all radiation and conduction losses.

$$h_C = \frac{q_C}{A_C(t_C - t_a)} \qquad (28)$$

where

h_C = fictitious heat transfer coefficient of Probe C

A_C = convection area which was assumed to be the exposed area of the thermistor and the copper washers

t_C = temperature measured by the washer thermistor

A relation between the fictitious heat transfer coefficient and the actual heat transfer coefficient would then consist of a calibration of Probe C.

CHAPTER VII

ANALYSIS OF EXPERIMENTAL DATA

When a thermistor is supplied with a certain power input in still air, it reaches an equilibrium temperature. If the transfer of heat is increased from the thermistor at a given heat input the temperature of the thermistor will drop. Because of the characteristics of thermistors, the resistance of the thermistor increases with the decreasing temperature, and the equilibrium value of the resistance will be higher than it was prior to the change. If the voltage is held constant across the thermistor the current flowing through the thermistor will thus decrease, and the power supplied to the thermistor will be less. If the voltage across the thermistor is not held constant both the voltage and current will change, but will do so in such a manner that the power input to the thermistor decreases. The heated thermistor probes followed these characteristics. In all the measurements the voltage and current were allowed to adjust as the heat transfer coefficient to which the probes were exposed was changed.

Correlations were made first to determine if Probe B could be used directly to determine local heat transfer rates, and then made to see if the average heat transfer

coefficients measured by Probe B could be related to the average heat transfer coefficient measured by Probe A.

In the analysis of the data for Probe C, correlations relating the fictitious heat transfer coefficient measured by Probe C to the heat transfer coefficients measured by Probe A were made.

Probe B

Analysis of the experimental data for Probe B indicates that the heat transfer coefficient calculated from equation (25)

$$h_B = \frac{q_B}{A_B (t_B - t_a)} \qquad (25)$$

is many times higher than that measured by Probe A, as can be seen by Figure 8.

There are two possible explanations for this. First, the heat conducted into the probe is large. This means that of the total heat input to the thermistor, only a small fraction is removed by convection from the measured area of the hole in which the thermistor is embedded. In order to use the measured area of the hole as a basis of calculating a heat transfer coefficient a q_B much less than the total would have to be used.

Another explanation for the large value of heat transfer coefficient obtained can be made from boundary layer

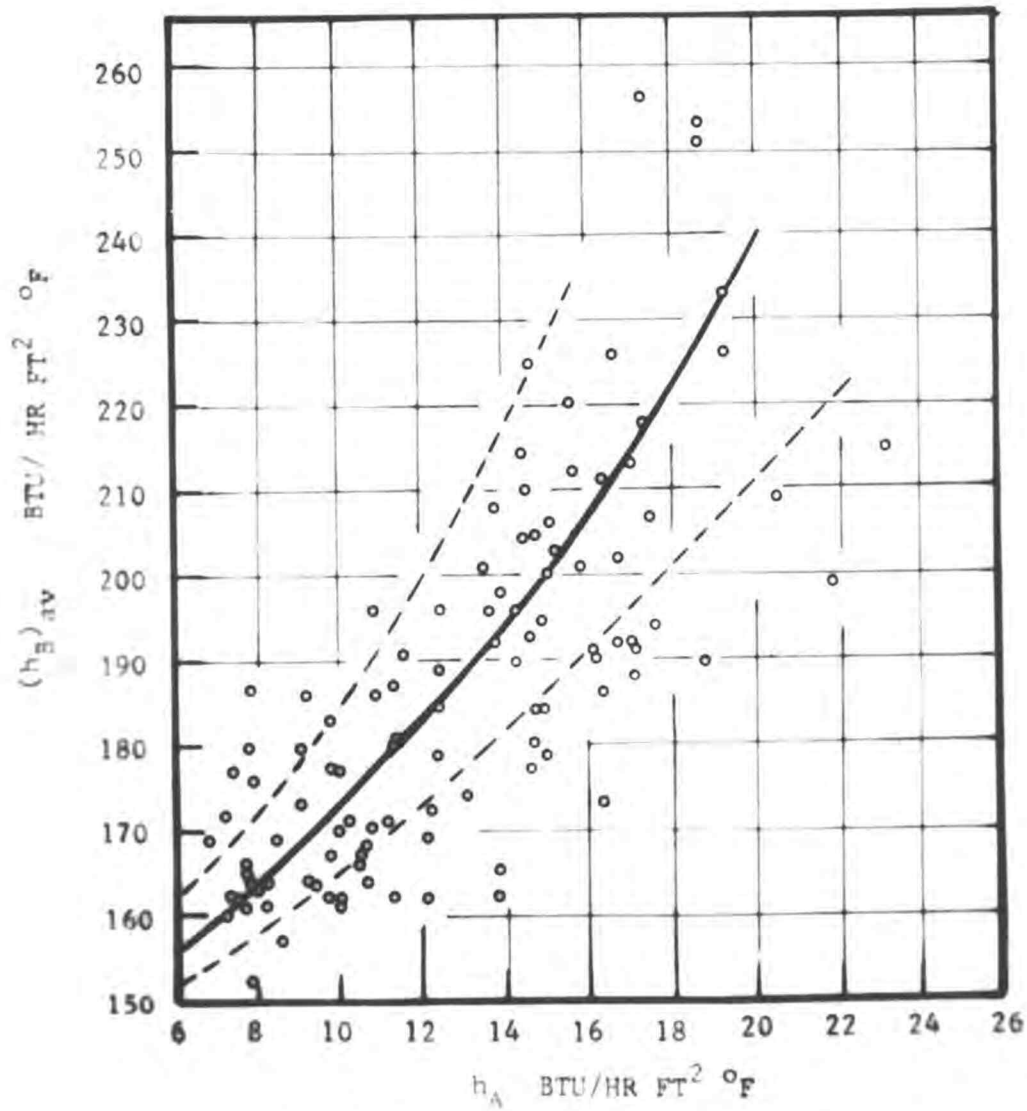

PROBE A HEAT TRANSFER COEFFICIENT VERSUS
PROBE B HEAT TRANSFER COEFFICIENT

FIGURE 8

theory. It is known that local heat transfer coefficients measured at the leading portion of a heating surface are larger than those measured at some distance downstream. An analytical expression has been developed by Rubesin (10) for flow over a flat plate having a stepwise surface-temperature discontinuity. At a constant flow rate for a given fluid, the heat transfer coefficient is related to the distance downstream from the starting point of the heating surface by

$$h_x = K\, x^{-1/5} \left[1 - (x_o/x)^{39/40}\right]^{-7/39} \qquad (29)$$

where

K = a constant dependent upon the fluid and the flow rate

x_o = distance from the leading edge of the plate to where the heating begins

x = distance from the leading edge of the plate where the local heat transfer coefficient is measured

In attempting to measure a local heat transfer coefficient by a small heated area such as an embedded thermistor bead, the term x_o/x would be very close to unity. Hence, the local heat transfer coefficient existing at this thermistor would be quite large. This heat transfer coefficient

would be much larger than that measured by Probe A under the same condition of flow and position.

A rigorous mathematical analysis taking into account all of the many factors affecting the heat transfer coefficient from an embedded thermistor bead would lead to very complicated differential equations. As an alternative, the data were analyzed by comparing the results with Probe A in an attempt to interpret the data from Probe B so that it could be used to measure representative coefficients in the exchanger.

Variation of heat transfer coefficient measured by Probe A with those measured by Probe B. Figure 8 shows a plot of average heat transfer coefficient of Probe B

$$(h_B)_{av} = 1/7 \sum_{1}^{7} h_B \qquad (30)$$

as a function of average heat transfer coefficient measured by Probe A. The average heat transfer coefficient from Probe B was calculated from equation (30). The solid line in Figure 8 passes through, approximately, midway between the widely scattered points. This represents an approximate calibration curve of Probe B compared to Probe A. In using Probe B values of h_A would be obtained from values of $(h_B)_{av}$ and could be determined through the use of the curve. The broken lines represent a $\pm$ 20 per cent deviation from

the curve in terms of h_A. These curves include 60 per cent of all the points.

These results indicate that Probe B is not satisfactory for measuring local rates of heat transfer. It is relatively insensitive to changes in h_A. It was noted during the experiment that a change of two in h_A caused a current change of only 0.05 milliamperes, and the milliammeter could only be read to only ± 0.01 milliamperes. This represents an error in $(h_B)_{av}$ of ± 6 per cent, and accounts somewhat for the considerable scattering of data. The insensitivity of Probe B is also seen from Figure 8 in which for a change in $(h_B)_{av}$ 150 to 240 (60 per cent), h_A changes from 6 to 20 (233 per cent).

It is therefore concluded that the use of thermistors embedded in a surface is not satisfactory for the measurement of local heat transfer coefficients when they are used as both the heat transfer surface and the temperature measuring element.

Variation of conduction and radiation losses with heat transfer coefficient. Figure 9 shows a plot of the average heat transfer coefficient as measured by Probe A against the ratio of conduction losses to total heat input for a typical thermistor bead (bead No. 1).

The ratio of losses to total heat input were calculated from the following equation.

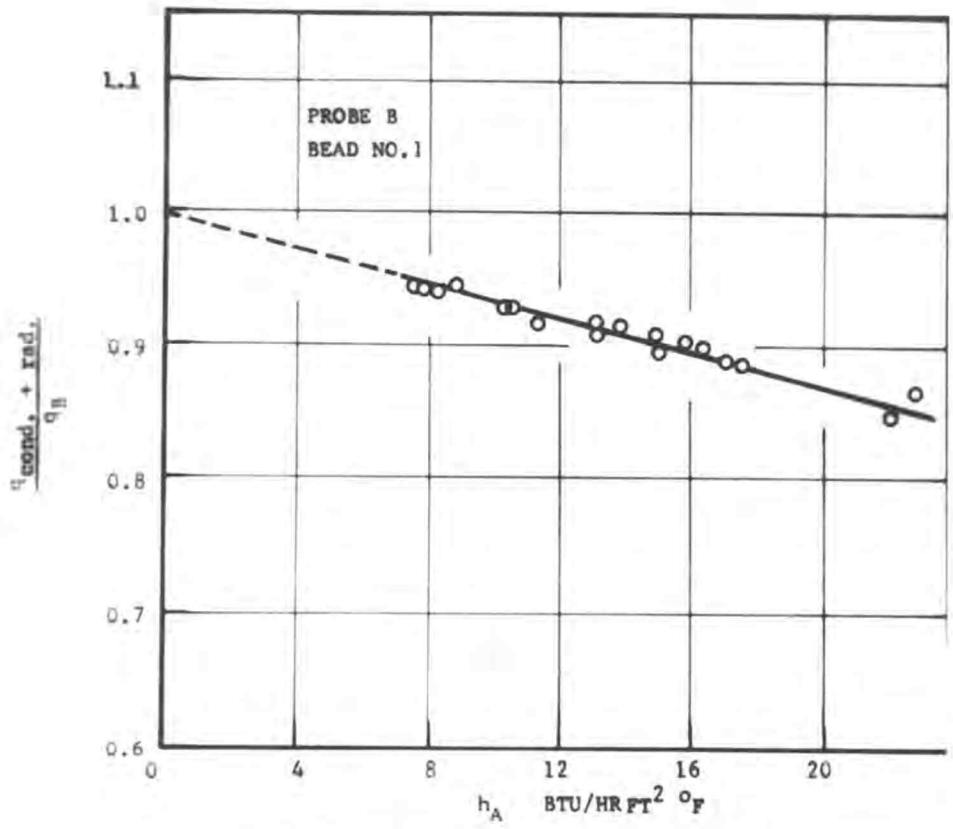

VARIATION OF CONDUCTION AND RADIATION LOSSES
WITH HEAT TRANSFER COEFFICIENT

FIGURE 9

$$\frac{q_{cond.\ +\ rad.}}{q_B} = 1 - \frac{h_A A_B (t_B - t_a)}{q_B} \qquad (31)$$

where

$q_{cond.\ +\ rad.}$ = heat loss by conduction and radiation

q_B = total measured heat input to the bead

The plot indicates that the conduction and radiation losses are high based on the coefficient measured by Probe A. They decrease with increasing heat transfer coefficient as would be expected from equation (31). When the heat transfer coefficient is equal to zero all heat would be transferred by conduction and radiation, and the ratio of these to total heat input would be unity. This result is obtained by extrapolating the line in Figure 9 to zero.

It must be emphasized that the amount of heat conducted into the plastic is not actually as large as that indicated because of the higher value of heat transfer coefficient on the thermistor to that existing on the foil.

Probe C

In relating the heat transfer coefficient measured by Probe A to the fictitious heat transfer coefficient calculated for Probe C, the fictitious heat transfer coefficient was based on the convection surface area of the thermistor

and the copper washers. This was done since the copper washers with their high thermal conductivity would have a surface temperature close to that of the washer thermistor. They would also tend to make the temperature distribution in the thermistor more uniform. The fictitious heat transfer coefficient was calculated from equation (28).

$$h_C = \frac{q_C}{A_C(t_C - t_a)} \qquad (28)$$

Since the thermistor indicated an average temperature, the temperature difference used is not the true difference between the air and the thermistor.

Variation of fictitious heat transfer coefficient with heat transfer coefficient measured by Probe A. Three sets of heat transfer coefficients were obtained in the wind tunnel tests as shown in Figure 10. The two curves and one point shown represent different initial heat inputs to the thermistor. The heat transfer coefficient was changed by changing the air flow rate in the wind tunnel.

It is apparent that the calibration of the washer thermistor is dependent upon heat input. This means that by holding h_A constant, h_C or its equivalent $q_C/ A_C(t_C - t_a)$ is not constant. This occurs because q_C is removed from the thermistor by convection, conduction, and radiation. At constant air flow rate, the heat transfer coefficient,

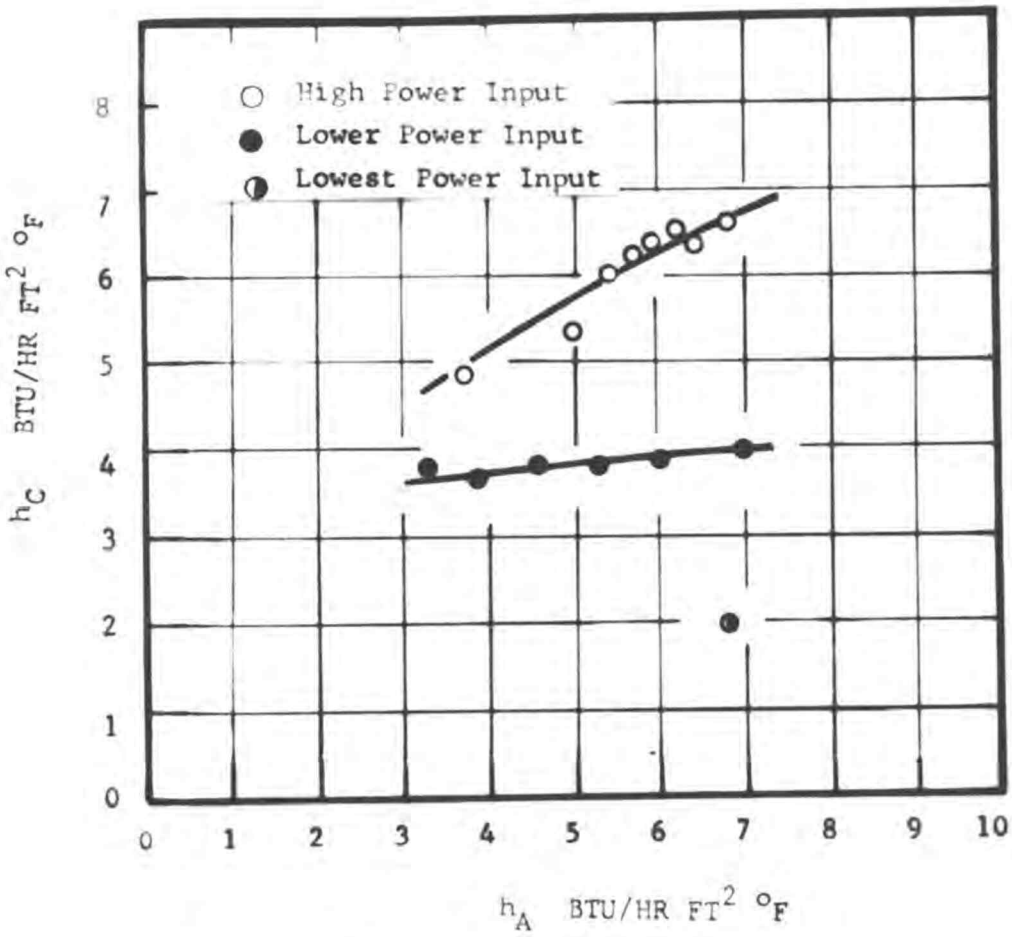

PROBE A HEAT TRANSFER COEFFICIENT VERSUS
PROBE C HEAT TRANSFER COEFFICIENT

FIGURE 10

h_A is independent of the heat input to the thermistor. As q_C increases $(t_C - t_a)$ increases (at constant h_A), and it might be expected therefore that a unique relationship between q_C and $(t_C - t_a)$ would exist at constant h_A. Thus also data on Probe C are plotted in Figure 11 as q_C versus $(t_C - t_a)$.

Variation in temperature difference with heat input at constant heat transfer coefficient. In Figure 11 the open circles represent data obtained in the model heat exchanger, and the closed circles are those obtained in the wind tunnel. The numbers on each point represent the values of h_A obtained from Probe A. A definite trend is evident in terms of h_A. The three lines on the lower right of Figure 11 represent constant values of h_A, and a calibration of the probe in the wind tunnel.

The data obtained in the model heat exchanger are not nearly as consistent as that obtained in the wind tunnel. From the heat exchanger data tentative calibration lines are drawn for values of 8.0, 10.0, 13.7, and 17.0. A number of points, however, are not in the correct position with respect to these values. In the wind tunnel the probes were exposed to a flowing stream which was relatively uniform, and the turbulence level was quite low. However, in the heat exchanger the probes were in a flowing

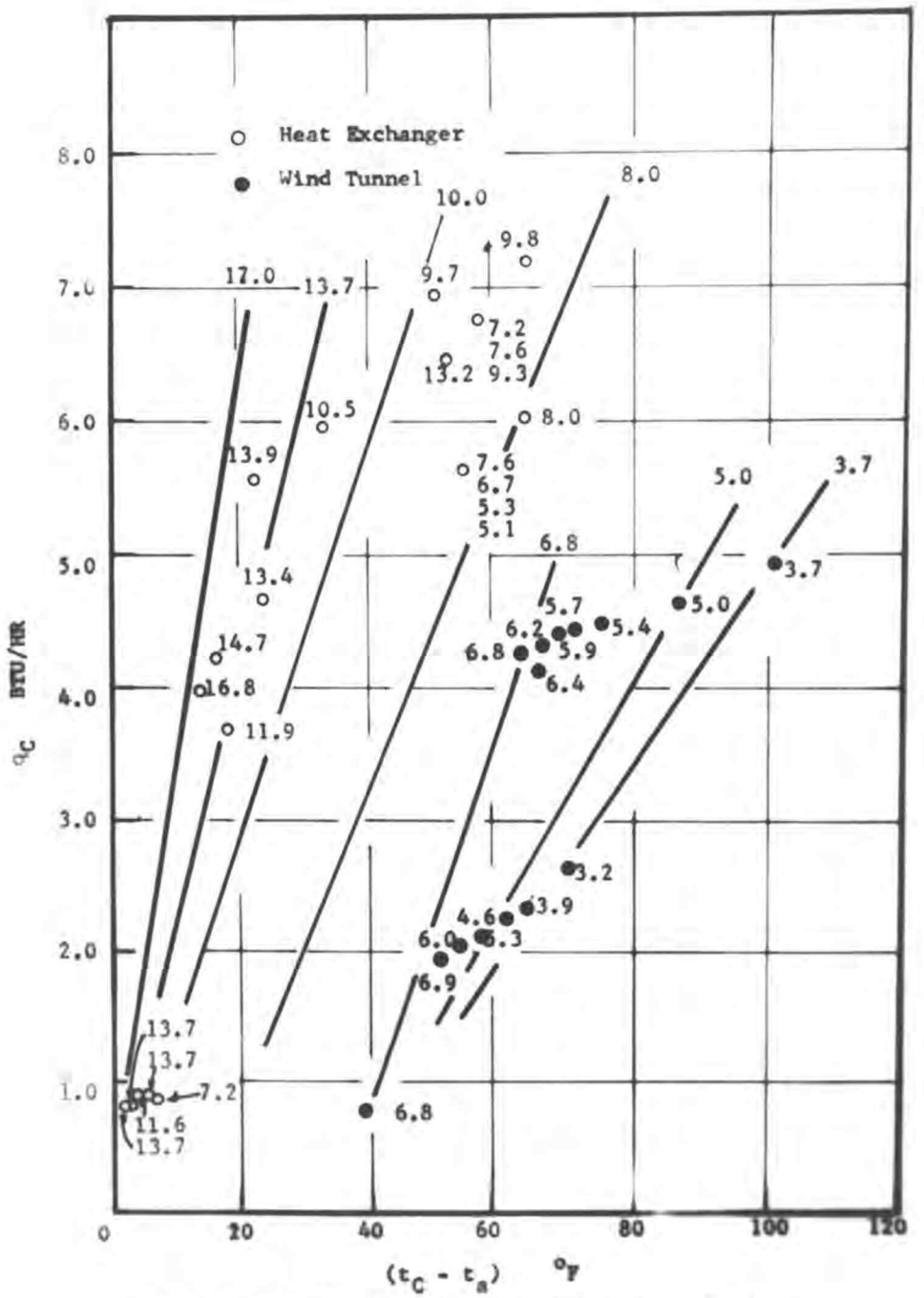

HEAT TRANSFERED BY PROBE C VERSUS TEMPERATURE DIFFERENCE AT CONSTANT HEAT TRANSFER COEFFICIENT

FIGURE 11

stream between two baffles, and there was considerable disturbance due to the baffles and adjacent tubes. Considerable variation of the local coefficient around the tube occurred if the tube was not exactly centered with respect to adjacent tubes and the baffle orifice. This could be detected and corrected for on Probe A. However, the variation around the tube could not be detected on Probe C, and in some cases it may have been eccentric with respect to adjacent tubes, and not in the same geometrical position as Probe A.

In the heat exchanger local coefficients change rapidly with distance, and the washer probe actually measures an average coefficient over its area. In positions where Probe A shows a change of local heat transfer coefficient, say from five to seven over a relatively small distance, Probe C indicates a relatively small change.

It is concluded that Probe C would be satisfactory for measurement of average coefficients around tubes in flow systems where the flow is uniform, and not greatly disturbed by adjacent surfaces or in positions where the coefficient is not changing rapidly over the surface. This situation existed in the wind tunnel experiments, and consistent calibration curves were obtained.

CHAPTER VIII

SUMMARY OF RESULTS

The investigation of the use of temperature sensitive resistors as a means of measuring local heat transfer coefficients has resulted in the following conclusions.

The two probes, Probe B and Probe C, have been compared with a standard heat transfer probe, Probe A, to determine their suitability for measuring local heat transfer coefficients. Comparisons were made at identical positions and flow rates.

Probe B, which consisted of a number of individual thermistors embedded around a cylinder, was shown to be too insensitive to changes in heat transfer coefficient measured by Probe A to obtain an accurate calibration. The result indicated that a large portion of the heat generated in the thermistors was lost by conduction rather than by convection assuming that Probe B and Probe A were exposed to the same heat transfer coefficient. It was therefore concluded that the use of heated thermistors embedded in a heat transfer sensing probe would not be suitable for use in measuring local values of heat transfer coefficients.

Probe C which used a relatively large heated washer thermistor was shown to be suitable for measurement of

average heat transfer coefficients around tubes in flow systems where the flow is uniform or where the coefficient is not changing rapidly with distance. Probe C would require calibration at several power inputs and ranges of known heat transfer coefficients. It would be advantageous to use Probe C under the above conditions, however, because of its fast response time, and the simplicity of its construction and the associated measuring system. Use would only be possible if a means of calibrating the probe were available.

It is concluded that the use of temperature sensitive resistors as used in Probes B and C would not be suitable for measurement of local heat transfer coefficients in a baffled heat exchanger.

NOMENCLATURE

A	Area of heat transfer, square feet
A_B	Measured area of Probe B
A_C	Measured area of Probe C
h	Local heat transfer coefficient
h_A	Average heat transfer coefficient measured by Probe A
h_B	Local heat transfer coefficient measured by Probe B
$(h_B)_{av}$	Average heat transfer coefficient measured by Probe B
h_C	Heat transfer coefficient measured by Probe C
I	Direct current supplied to thermistor
i	Direct current supplied to resistance ribbon
k	Thermal conductivity of resistance foil
P	Power, watts
q	Heat transferred, Btu/hr.
q_B	Heat transferred by a Probe B thermistor
q_C	Heat transferred by a Probe C thermistor
$q_{cond.}$	Heat loss by conduction
$q_{rad.}$	Heat loss by radiation
R	Resistance, ohms
S	Length of resistance ribbon
T	Temperature, ^oR
t_a	Air temperature, ^oF

t_B	Temperature of Probe B thermistor
t_C	Temperature of Probe C thermistor
w	Width of resistance ribbon
z	Thickness of resistance ribbon
α	Temperature coefficient of resistance
β	Constant characteristic of thermistor material
ρ	Specific resistance

BIBLIOGRAPHY

1. Ambrose, Tommy W. Local shell-side heat transfer coefficients in baffled tubular exchangers. Ph.D. thesis. Corvallis, Oregon State College, 1957. 183 numb. leaves.

2. Becker, C. B. Green and G. L. Pearson. Properties and uses of thermistors - thermally sensitive resistors. Electrical Engineering 65:711-725. 1946.

3. Dwyer, O. E. et al. Heat transfer rates for cross-flow of water through a tube bank at Reynolds numbers up to a million. 1952. 23 p. (U.S. Brookhaven National Laboratory BNL-1518) (Microcard)

4. Giedt, W. H. Investigation of variation of point unit heat-transfer coefficient around a cylinder normal to an air stream. Transactions of the American Society of Mechanical Engineers 71:375-381. 1949.

5. Gould, R. K. and W. L. Nyberg. Imbedded thermistor for boundary layer measurement. Acoustical Society of America Journal 31:249-250. 1959.

6. Hartwig, F. W., C. A. Bartch and H. McDonald. Miniaturized heat meter for steady-state aerodynamic heat-transfer measurements. Journal of the Aeronautical Sciences 24:239. 1957.

7. Knudsen, J. G. and Donald L. Katz. Fluid dynamics and heat transfer. New York, McGraw-Hill, 1958. 576 p.

8. McAdams, William H. Heat transmission. 3d ed. New York, McGraw-Hill, 1954. 532 p.

9. Narayanan, K. Local and over-all heat transfer coefficients in baffled heat exchangers. Ph.D. thesis. Corvallis, Oregon State College, 1962. 121 numb. leaves.

10. Rubesin, M. W. The effect of an arbitrary surface-temperature variation along a flat plate on the convective heat transfer in an incompressible turbulent boundary layer. Washington, 1951. 37 p. (U.S. National Advisory Committee for Aeronautics Technical Note 2345)

11. Schmidt, Ernst and Karl Wenner. Heat transfer over the circumference of a heated cylinder in transverse flow. Washington, 1943. 15 p. (U. S. National Advisory Committee for Aeronautics. Technical Memorandum No. 1050)

12. William, Peter Stanton. Heat transfer and pressure profiles in the vicinity of annular orifices. Master's thesis. Corvallis, Oregon State College, 1957. 86 numb. leaves.

13. Winding, C. C. and A. J. Cheney, Jr. Mass and heat transfer in tube banks. Industrial and Engineering Chemistry 40:1087-1093. 1948.

14. Zapp, George Michael, Jr. The effect of turbulence on local heat transfer coefficients around a cylinder normal to an air stream. Master's thesis. Corvallis, Oregon State College, 1950. 79 numb. leaves.

APPENDIX

Table I

CALIBRATION RESISTANCES AND TEMPERATURES

	Thermistor No.	Temperature ^{o}R	Resistance ohms	β ^{o}R
Probe A				
	1	560.0	59768	7750 ± 100
	2		60214	
	3		61437	
	4		64076	
	5		64076	
	6		66420	
	7		60054	
Air temperature	8		59768	
Probe B	1-8	560.0	58,000 ± 200	7750 ± 100
Probe C		538.9	482.7	7150 ± 100

Table II

MEASURED CONVECTION AREAS

	Thermistor No.	Average Diameter cm.	Area - $_2A_B$ ft.
Probe B - Hole Area			
	1	0.160	0.0000217
	2	0.143	0.0000171
	3	0.147	0.0000183
	4	0.140	0.0000165
	5	0.137	0.0000159
	6	0.150	0.0000159
	7	0.130	0.0000190
	8	No measurements made with this thermistor because of bad connection	
Probe C			A_C
		0.750	0.0102

Table III

PROBE B - CALIBRATION IN MODEL HEAT EXCHANGER

(1) Run No.		(2) 1	(3) 2	(4) 3	(5) 4	(6) 5	(7) 6	(8) 7	(9) t_a	(10)* h_A
399	t_B	73.88	79.61	72.84	73.88	73.88	75.87	72.84	60.33	15.77
	h_B	167.6	175.5	208.8	220.5	228.8	211.1	201.1		
400		73.88	78.70	72.84	74.89	74.89	76.84	74.89	60.33	14.75
		167.6	179.7	208.8	211.2	219.2	204.2	183.4		
401		74.89	80.93	73.36	75.87	75.38	77.31	74.89	60.33	16.16
		160.6	170.3	203.6	203.4	214.9	201.1	183.4		
402		75.87	81.36	73.88	75.87	75.87	78.25	74.89	60.33	16.93
		157.7	171.2	203.2	207.4	215.2	199.0	187.2		
403		77.78	86.24	76.84	77.78	77.31	80.49	76.84	60.33	14.60
		147.8	157.9	180.7	194.4	204.7	187.7	174.0		
404		78.70	89.22	78.70	78.70	78.70	82.21	77.78	60.59	12.97
		145.9	154.3	173.1	192.0	199.2	183.2	171.4		
405		78.70	92.69	80.49	80.49	82.21	86.24	78.70	60.59	10.37
		145.9	150.4	165.2	183.2	183.2	171.6	166.7		

*Baffle geometry, tube pitch, baffle orifice size, exact probe positions, and individual local heat transfer coefficients are listed by Narayanan (9) under the corresponding run numbers.

Table III (Continued)

(1)	(2)	(3)	(4)	(5)	(6)	(7)	(8)	(9)	(10)
406	79.61 142.4	98.34 147.4	83.05 156.6	82.21 176.5	83.05 180.3	87.00 169.9	79.61 162.6	60.59	8.19
407	79.65 128.7	80.58 159.6	80.58 149.1	80.58 165.4	81.49 168.2	85.78 156.2	79.65 147.0	60.59	7.81
408	77.73 135.9	79.65 163.3	78.70 156.6	78.70 173.7	79.65 175.6	84.12 160.1	78.70 150.8	60.59	7.47
409	80.52 135.8	81.39 169.0	81.83 156.5	80.96 176.9	81.83 180.1	87.48 164.9	80.07 156.8	60.59	7.35
410	79.63 135.5	80.54 168.1	80.54 157.1	80.54 174.2	80.98 178.9	86.80 162.1	79.63 154.7	60.59	7.72
411	77.76 142.9	80.54 168.1	78.70 164.7	78.70 182.7	79.63 184.9	83.15 171.3	77.76 163.2	60.59	10.18
412	74.89 166.9	79.61 180.7	73.88 207.2	75.87 210.9	76.84 211.2	77.78 204.8	74.89 190.6	60.59	13.73
413	75.87 160.3	79.61 180.7	73.88 207.2	76.84 203.6	76.84 211.2	77.78 204.8	74.89 190.6	60.59	12.91
414	74.33 166.9	79.16 178.4	74.33 197.9	75.84 206.0	76.33 209.9	78.24 197.0	83.52 146.0	60.59	16.25
415	74.33 166.9	80.07 174.3	74.33 197.9	76.33 202.3	76.33 209.9	77.77 199.9	74.33 190.6	60.59	16.04

Table III (Continued)

(1)	(2)	(3)	(4)	(5)	(6)	(7)	(8)	(9)	(10)
416	74.84 163.2	80.07 174.3	73.82 202.8	76.33 202.3	77.30 203.0	78.24 197.0	74.33 190.6	60.59	18.75
417	74.33 166.9	80.07 174.3	74.33 197.9	76.33 202.3	77.30 203.0	80.07 187.4	74.84 186.4	60.59	17.09
418	75.80 153.0	80.54 168.1	75.30 185.1	77.76 188.0	77.76 195.0	83.99 168.8	78.70 158.7	60.59	16.25
419	77.76 142.9	82.30 161.8	77.76 169.5	78.70 182.7	80.54 180.8	84.81 166.6	79.63 154.7	60.59	13.68
420	77.76 142.9	82.30 161.8	78.70 164.7	79.63 178.2	81.43 177.2	86.41 162.9	80.54 151.3	60.59	12.02
421	78.70 138.9	82.30 161.8	77.76 169.5	79.63 178.2	82.30 174.0	86.41 162.9	80.54 151.3	60.59	9.65
422	79.63 135.5	81.43 164.8	77.76 169.5	78.70 182.7	80.54 180.8	87.19 161.4	79.63 154.7	60.59	9.19
423	79.63 135.5	82.30 161.8	78.70 164.7	79.63 178.2	81.43 177.2	87.96 160.0	79.63 154.7	60.59	8.93
424	79.63 135.5	81.43 164.8	78.70 164.7	78.70 182.7	81.43 177.2	87.96 160.0	79.63 154.7	60.59	8.96
425	79.63 135.5	82.30 161.8	78.70 164.7	79.63 178.2	81.43 177.2	87.96 160.0		60.59	9.51

Table III (Continued)

(1)	(2)	(3)	(4)	(5)	(6)	(7)	(8)	(9)	(10)
426	78.23	81.01	78.23	79.18	80.10	84.47	78.23	60.59	11.20
	137.4	162.1	162.9	175.8	178.1	163.3	156.9		
427	75.25	80.10	74.21	76.27	76.27	77.26	75.25	60.59	14.60
	152.5	165.6	189.3	192.8	200.1	193.3	174.2		
428	74.79	80.54	74.79	76.79	76.79	77.76	74.79	60.59	14.67
	159.5	168.1	189.2	194.1	201.4	195.0	182.2		
429	71.78	76.84	69.58	71.78	72.84	70.70	71.78	59.08	16.13
	172.6	179.8	233.1	227.1	223.9	250.1	197.2		
430	70.70	75.87	69.58	72.84	72.84	71.78	71.78	59.08	14.41
	183.2	185.2	233.1	215.7	223.9	235.6	197.2		
431	71.78	76.84	71.78	72.84	72.84	71.78	72.84	59.08	16.62
	172.6	179.8	204.7	215.7	223.9	235.6	187.3		
432	72.32	76.84	71.78	72.84	73.36	72.84	72.84	59.08	21.76
	168.1	179.8	204.7	215.7	218.8	223.9	187.3		
433	75.34	77.30	73.29	74.33	75.34	75.84	74.84	59.08	14.62
	145.0	173.1	186.0	197.8	197.9	194.6	168.5		
434	76.33	78.24	75.84	76.33	77.30	77.30	76.33	59.33	11.95
	142.4	171.0	171.6	187.3	188.7	188.7	162.6		
435	75.34	78.24	75.34	76.81	78.70	78.24	76.81	59.33	10.11
	147.2	171.0	174.5	184.5	181.7	183.9	160.2		

Table III (Continued)

(1)	(2)	(3)	(4)	(5)	(6)	(7)	(8)	(9)	(10)
436	76.79 136.9	78.23 166.8	76.30 164.9	76.79 180.1	78.70 177.3	78.70 177.3	77.76 152.1	59.33	8.31
437	77.30 138.3	78.24 171.0	77.30 164.0	77.77 179.5	79.16 179.7	80.07 176.1	78.24 153.9	59.33	7.49
438	77.76 133.1	78.70 164.8	76.79 162.4	77.76 175.1	79.63 173.4	80.09 171.7	79.17 146.7	59.33	7.20
439	75.84 144.7	77.30 175.5	75.34 174.5	76.33 187.3	78.24 183.9	78.24 183.9	77.30 157.9	59.33	7.20
440	75.87 148.1	77.78 177.4	76.84 170.3	75.87 194.8	77.78 190.8	77.78 190.8	76.84 164.0	59.33	7.93
441	74.33 152.9	77.30 175.5	76.33 168.8	75.34 193.6	76.81 191.4	76.33 194.3	75.34 168.1	59.33	9.81
442	75.34 147.2	76.33 180.7	71.14 211.0	72.23 220.8	73.29 217.9	71.14 242.9	72.23 191.7	59.33	13.46
443	71.60 169.3	76.79 173.7	72.69 189.9	72.69 210.6	73.75 208.4	71.60 231.0	71.60 193.3	59.33	12.33
444	70.03 178.4	73.29 192.5	70.03 211.5	72.23 208.9	72.23 216.8	70.03 243.5	70.59 197.2	58.60	14.98
445	69.91 179.1	74.27 183.7	71.60 193.0	72.69 203.2	73.22 206.0	70.48 236.1	71.60 185.9	58.84	13.85

Table III (Continued)

(1)	(2)	(3)	(4)	(5)	(6)	(7)	(8)	(9)	(10)
446	71.60 162.8	74.79 180.2	71.60 193.0	73.22 198.5	72.69 210.8	71.04 228.7	72.69 176.4	58.84	16.58
447	71.60 162.8	74.79 180.2	71.60 193.0	72.69 203.2	72.69 210.8	71.04 228.7	72.15 180.9	58.84	17.53
448	74.33 148.0	76.33 175.6	73.82 179.1	74.33 194.7	75.34 194.9	74.84 198.3	74.84 166.0	58.84	14.98
449	74.84 145.3	76.33 175.6	75.84 166.6	76.33 182.0	78.24 179.3	78.24 179.3	76.33 158.1	58.84	11.93
450	75.30 141.6		76.79 160.1	77.28 175.1	78.70 175.0	76.79 184.3	76.30 156.5	59.08	10.05
451	75.30 141.6	76.79 171.3	76.79 160.1	77.76 172.8	78.70 175.0	77.76 179.3	76.30 156.5	59.08	9.13
452	75.80 139.2	76.79 171.3	76.79 160.1	77.76 172.8	79.63 171.3	78.70 175.0	76.79 154.2	59.08	8.22
453	75.80 139.2	76.79 171.3	76.79 160.1	77.28 175.1	78.70 175.0	78.23 177.1	77.28 152.0	59.08	7.79
454	75.80 139.2	76.79 171.3	76.79 160.1	77.76 172.8	79.63 171.3	78.70 175.0	77.28 152.0	59.08	7.98
455	76.33 140.4	77.30 173.1	77.30 161.8	78.24 174.9	79.16 177.5	77.77 183.8	77.30 155.8	59.08	8.36

Table III (Continued)

(1)	(2)	(3)	(4)	(5)	(6)	(7)	(8)	(9)	(10)
456	77.30	78.24	80.07	78.24	79.16	77.30	76.33	59.08	10.28
	136.4	168.8	151.2	174.9	177.5	186.2	160.3		
457	72.23	79.16	72.23	73.82	74.33	72.23	73.29	59.08	14.03
	164.7	165.0	195.3	201.9	205.3	224.8	179.2		
458	73.29	76.33	71.14	73.29	74.33	71.69	72.23	59.08	13.55
	156.9	178.1	206.7	206.3	205.3	231.0	188.1		
527	71.78	70.70	71.78	73.88	73.88	71.78	72.84	59.58	22.95
	179.6	242.9	213.0	213.5	221.6	245.2	194.3		
528	69.58	68.43	68.43	71.78	71.78	69.58	70.70	58.60	16.50
	187.9	257.9	241.0	218.7	226.9	256.4	200.9		
529	70.70	69.58	69.58	71.78	71.78	70.70	70.70	59.08	19.20
	183.2	249.5	233.1	227.1	235.6	250.1	209.3		
530	71.24	70.70	72.84	71.78	71.78	70.70	71.78	58.60	17.19
	170.8	223.2	187.9	218.7	226.9	240.1	189.9		
531	71.78	70.70	72.32	73.88	73.88	71.78	72.84	59.08	15.10
	172.6	232.5	199.4	206.4	214.2	235.6	187.3		
532	73.88	71.78	73.88	74.89	75.87	74.89	74.89	58.99	12.25
	155.9	217.4	184.9	197.3	198.0	204.8	171.4		

Table III (Continued)

(1)	(2)	(3)	(4)	(5)	(6)	(7)	(8)	(9)	(10)
533	74.89	72.84	74.89	74.89	75.87	75.87	73.88	59.08	11.14
	151.0	208.2	179.0	198.6	199.2	199.2	179.2		
534	75.87	73.88	75.87	75.87	76.36	75.87	75.87	59.08	11.33
	145.9	199.1	173.1	191.9	196.1	199.2	166.7		
535	75.87	73.88	76.36	75.87	76.36	75.87	75.87	59.08	11.17
	145.9	199.1	170.4	191.9	196.1	199.2	166.7		
536	70.70	69.58	69.58	71.78	71.78	70.70	71.78	59.08	15.65
	183.2	249.5	233.1	227.1	235.6	250.1	197.2		
537	72.23	72.23	74.33	73.29	73.29	72.23	73.29	59.08	14.15
	164.7	209.0	178.4	206.3	214.1	224.8	179.2		
538	73.88	73.88	74.89	73.88	74.89	73.88	74.89	59.08	15.93
	156.9	199.1	179.0	206.4	206.1	214.2	172.4		
539	75.87	72.84	72.84	73.88	74.89	73.88	74.89	59.08	16.96
	145.9	208.2	194.5	206.4	206.1	214.2	172.4		
540	75.87	74.89	75.87	74.89	75.87	73.88	75.87	59.08	14.82
	145.9	191.6	173.1	198.6	199.2	214.2	166.7		
541	78.70	75.87	77.78	77.78	78.70	76.84	77.78	59.08	11.05
	134.7	185.2	163.6	181.4	183.9	193.3	157.6		
542	77.78	77.31	78.70	77.78	78.70	78.25	77.78	59.08	10.48
	137.9	177.3	159.8	181.4	183.9	186.0	157.6		

Table III (Continued)

(1)	(2)	(3)	(4)	(5)	(6)	(7)	(8)	(9)	(10)
543	78.70	76.84	78.70	77.78	79.61	78.70	77.78	59.08	9.76
	134.7	179.8	159.8	181.4	180.1	183.9	157.6		
544	77.78	76.84	76.84	77.78	78.70	77.78	77.78	59.08	10.70
	137.9	179.8	168.0	181.4	183.9	188.3	157.6		
545	73.88	73.88	72.84	73.88	74.89	73.88	73.88	59.08	14.48
	156.9	199.1	194.5	206.4	206.1	214.2	179.2		
546	73.75	72.69	73.75	74.79	75.80	73.75	74.79	59.58	25.16
	155.4	207.1	184.2	195.8	195.8	212.0	170.1		
547	71.14	70.03	70.59	72.23	72.23	71.14	72.23	59.08	15.58
	174.3	236.4	213.4	216.6	224.8	237.9	188.1		
548	71.14	70.03	70.59	72.23	72.23	71.14	72.23	59.08	16.90
	174.3	236.4	213.4	216.6	224.8	237.9	188.1		
549	71.69	70.03	71.14	72.77	73.29	72.23	72.23	59.08	17.35
	169.3	236.4	206.7	211.2	214.1	224.8	188.1		
550	73.29	70.03	73.29	74.33	75.34	74.33	74.33	59.08	13.78
	156.9	236.4	186.0	197.8	197.9	205.3	171.8		
551	75.34	71.14	76.33	76.33	76.33	75.34	76.33	59.58	10.69
	149.5	230.7	171.3	190.0	197.2	204.1	165.0		
552	75.87	71.78	76.84	75.87	77.31	76.84	76.84	59.58	9.12
	150.4	227.9	172.8	197.8	196.0	198.9	166.4		

Table III (Continued)

(1)	(2)	(3)	(4)	(5)	(6)	(7)	(8)	(9)	(10)
553	74.89 151.0	73.88 199.1	75.87 173.1	74.89 198.6	75.87 199.2	75.87 199.2	75.87 166.7	59.08	9.67
554	74.89 151.0	72.84 208.2	74.89 179.0	74.39 202.3	74.89 206.1	73.88 214.2	73.88 179.2	59.08	11.53
555	71.78 172.6	71.78 219.1	71.78 204.7	72.84 215.7	72.84 223.9	71.78 235.6	71.78 197.2	59.08	14.40
556	72.84 167.0	71.78 223.4	71.78 208.8	71.78 231.5	72.84 227.9	71.78 240.3	71.78 201.1	59.33	14.28
557	72.84 167.0	72.32 217.4	73.88 189.2	74.89 201.7	73.88 217.8	72.84 227.9	73.88 182.2	59.33	14.93
558	73.36 163.1	72.32 217.4	73.36 193.4	73.36 214.5	73.36 222.6	72.32 233.8	72.84 190.7	59.33	15.35
559	76.36 143.7	73.88 199.1	75.38 175.9	74.89 198.6	75.87 199.2	74.49 209.1	74.89 172.4	59.08	12.36
560	76.84 141.6	73.88 199.1	77.78 163.6	76.84 186.3	76.84 193.3	75.87 199.2	74.89 172.4	59.08	12.26
561	76.84 141.6	74.89 191.6	77.78 163.6	75.87 191.9	76.84 193.3	75.87 199.2	75.87 166.7	59.08	9.83
562	77.78 137.9	75.87 185.2	79.61 156.5	77.78 181.4	78.70 183.9	77.78 188.3	77.78 157.6	59.08	9.84

Table III (Continued)

(1)	(2)	(3)	(4)	(5)	(6)	(7)	(8)	(9)	(10)
563	76.84	76.84	77.78	77.78	77.78	77.78	76.84	59.08	12.05
	141.6	179.8	163.6	181.4	188.3	188.3	161.8		
564	74.89	72.84	72.84	73.88	74.89	72.84	73.88	59.08	14.08
	151.0	208.2	194.5	206.4	206.1	223.1	179.2		
807	70.14	70.14	69.01	70.14	69.58	70.70	70.70	60.23	18.64
	211.5	268.4	274.3	278.1	301.2	277.5	232.2		
808	70.70	70.70	69.58	70.70	69.58	70.70	71.24	60.23	17.02
	203.3	258.1	261.7	267.4	301.2	277.5	224.0		
809	71.78	71.78	71.78	71.78	71.24	71.24	71.78	60.08	19.11
	187.3	237.7	222.1	246.4	264.1	264.1	213.9		
810	72.84	72.84	72.32	72.84	71.78	72.84	73.36	60.08	15.45
	176.8	224.4	215.6	232.6	255.7	241.3	196.8		
811	73.88	73.88	72.84	73.36	73.88	74.39	74.39	60.08	20.92
	168.2	213.5	209.7	226.6	229.6	224.5	187.9		
812	74.89	74.39	73.88	74.89	73.36	74.89	74.89	59.58	10.71
	155.8	201.7	192.5	205.0	226.6	212.7	178.0		
813	75.87	75.87	75.87	76.84	76.36	81.36	75.87	59.58	9.0
	150.4	190.8	178.3	191.6	201.9	177.8	171.7		

Table III (Continued)

(1)	(2)	(3)	(4)	(5)	(6)	(7)	(8)	(9)	(10)
814	75.87 150.4	75.38 194.2	74.89 184.8	75.87 197.8	76.36 201.9	74.89 212.7	76.36 169.0	59.58	7.86
815	76.84 145.7	75.87 190.8	76.36 175.4	76.84 191.6	77.78 193.4	76.84 198.9	76.36 169.0	59.58	7.84
816	76.84 145.7	76.84 184.9	77.78 168.0	76.84 191.6	77.78 193.4	77.78 193.4	76.84 166.4	59.58	7.48
817	77.78 137.9	78.25 173.0	77.78 163.6	78.25 179.3	77.78 188.3	77.78 188.3	78.25 155.7	59.08	6.82
818	77.31 136.1	77.31 172.7	77.78 159.4	76.84 181.3	77.31 185.8	77.78 183.5	79.61 147.2	58.60	7.74
819	75.38 128.1	75.38 162.5	74.89 153.9	75.87 166.4	75.38 174.8	75.87 172.6	75.87 144.5	56.50	8.57
820	73.88 122.7	73.36 157.9	73.88 145.6	73.88 161.4	74.39 165.4	73.88 167.5	73.88 140.2	54.97	12.80
821	73.88 134.6	75.87 161.7	71.78 171.6	75.87 167.5	74.39 181.0	74.89 178.4	75.38 147.3	56.64	13.76

Table IV

PROBE C - CALIBRATION IN MODEL HEAT EXCHANGER

(1) Run No.	(2) t_C	(3) t_a	(4) t_C-t_a	(5) q_C	(6) h_C	(7)* h_A
603	60.38	58.36	2.02	0.836	40.57	13.72
604	60.38	58.36	2.02	0.836	40.57	11.75
605	60.92	58.60	2.31	0.848	35.87	13.75
606	61.18	58.60	2.58	0.866	32.93	15.0
607	62.49	58.60	2.89	0.884	22.26	13.7
608	64.19	58.60	5.59	0.911	15.97	11.6
609	64.19	58.60	5.59	0.911	15.97	10.0
610	64.89	58.60	6.38	0.930	14.28	7.15
611	65.76	58.60	7.16	0.949	12.98	6.75
612	65.76	58.60	7.16	0.949	12.98	6.50
613	66.04	58.60	7.44	0.942	12.40	7.15
614	64.87	58.60	6.27	0.914	14.29	7.45
615	63.28	58.60	4.68	0.889	18.63	8.5
616	61.73	58.60	3.11	0.835	26.33	10.9
617	62.14	58.60	3.54	0.863	23.89	10.6
1056	104.78	72.46	32.32	6.08	18.44	10.54
1057	121.33	72.08	49.24	6.99	13.92	9.75
1058	134.98	72.16	62.82	6.12	9.54	8.05
1059	125.52	71.86	53.65	5.68	10.39	7.65
1060	126.01	72.31	53.70	5.74	10.48	6.71
1061	125.80	72.31	53.49	5.65	10.36	5.26
1062	125.03	72.68	52.34	5.63	10.54	5.10
1063	89.85	72.38	17.47	3.67	20.60	11.40
1064	92.98	72.21	21.77	5.61	25.29	13.86
1065	126.13	71.06	55.06	6.82	12.14	7.17
1066	126.13	71.13	54.99	6.82	12.15	7.57
1067	124.71	71.13	53.57	6.76	12.38	9.37
1068	133.40	70.92	62.48	7.25	11.37	9.77
1069	121.19	70.85	50.34	6.48	12.63	13.22
1070	93.79	70.78	23.01	4.73	20.15	13.42
1071	86.90	70.99	15.90	4.24	26.15	14.73
1072	84.20	70.42	13.77	4.04	28.80	16.86

*Baffle geometry, tube pitch, baffle orifice size, exact probe positions, and individual local heat transfer coefficients are listed by Narayanan (9) under the corresponding run numbers.

Table V

PROBE C - CALIBRATION IN WIND TUNNEL

(1) Run No.	(2) t_C	(3) t_a	(4) $t_C - t_a$	(5) q_C	(6) h_C	(7) h_A
1	154	53.48	100.52	5.02	4.87	3.70
2	139	52.42	86.58	4.60	5.35	4.99
3	127	52.59	74.41	4.53	6.00	5.42
4	123	52.63	70.37	4.44	6.22	5.68
5	122	52.70	69.30	4.48	6.37	5.90
6	119	52.99	66.01	4.30	6.48	6.23
7	118	52.94	65.06	4.20	6.25	6.40
8	117	52.86	64.14	4.30	6.59	6.83
9	92	53.08	39.92	0.78	1.96	6.83
10	127	58.07	68.93	2.68	3.80	3.16
11	119	56.23	62.77	2.36	3.68	3.92
12	115	55.52	59.48	2.28	3.79	4.61
13	111	54.45	56.55	2.15	3.76	5.33
14	107	55.59	52.41	2.08	3.85	6.05
15	105	55.40	49.60	2.00	3.92	6.87

Table VI

PROBE A - HEAT TRANSFER COEFFICIENTS IN WIND TUNNEL CALIBRATION

Run No.	Thermistor Number (1)	(2)	(3)	(4)	(5)	(6)	(7)	(8)
	h_1	h_2	h_3	h_4	h_5	h_6	h_7	h_A
1	3.95	3.84	3.87	3.73	3.36	3.45	3.69	3.70
2	5.30	5.22	5.19	4.90	4.45	4.73	5.08	4.99
3	5.80	5.66	5.59	5.30	4.88	5.20	5.54	5.42
4	6.19	6.08	5.95	5.69	5.73	4.94	5.15	5.68
5	6.05	5.05	5.57	5.98	6.09	6.10	6.01	5.90
6	6.42	5.80	5.88	6.34	6.39	6.45	6.36	6.23
7	6.62	6.01	6.04	6.45	6.59	6.61	6.50	6.40
8	7.14	6.47	6.49	6.88	7.07	7.19	6.56	6.83
9	6.93	6.76	7.10	7.06	6.44	6.58	6.97	6.83
10	3.14	3.04	3.22	3.30	3.10	3.13	3.23	3.16
11	3.87	3.86	4.12	4.19	3.82	3.74	3.82	3.92
12	4.59	4.55	4.85	4.93	4.46	4.38	4.53	4.61
13	5.33	5.31	5.62	5.57	5.10	5.08	5.26	5.33
14	6.09	6.03	6.31	6.31	5.85	5.79	5.99	6.05
15	6.88	6.81	7.18	7.13	6.51	6.67	6.93	6.87